



TITLE:

<Advanced Research Center for Beam Science>Electron Microscopy and Crystal Chemistry

AUTHOR(S):

CITATION:

<Advanced Research Center for Beam Science>Electron Microscopy and Crystal Chemistry. ICR Annual Report 2011, 18: 48-49

ISSUE DATE:

2011

URL:

<http://hdl.handle.net/2433/154951>

RIGHT:

Advanced Research Center for Beam Science – Electron Microscopy and Crystal Chemistry –

<http://eels.kuicr.kyoto-u.ac.jp:8080/Root/English>



Assoc Prof
KURATA, Hiroki
(D Sc)



Assist Prof
OGAWA, Tetsuya
(D Sc)



Assist Prof
NEMOTO, Takashi
(D Sc)



Res*
MORIGUCHI, Sakumi
(D Sc)

* Re-employed Staff

Students

KIYOMURA, Tsutomu (RF)
SHINODA, Yasuhiro (D3)
SAITO, Hikaru (D1)

ASO, Ryotaro (D1)
KARIYA, Ayuta (M2)

UMEMURA, Kayo (M2)
OGIMOTO, Mao (M1)

Visitors

Dr WIENGMOON, Amporn
Dr LO, Shen-Chuan
Prof CHEN, Cheng-Hsuan
Dr KRIVANEK, Ondrej

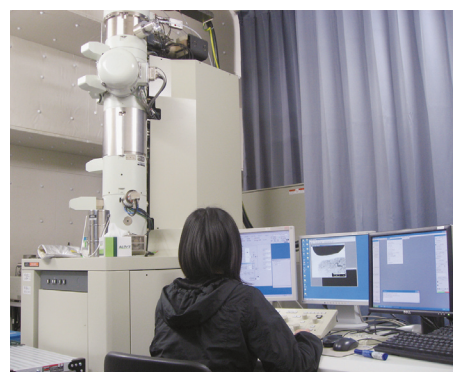
Naresuan University, Thailand, 5–30 April
Industrial Technology Research Institute, Taiwan, 23–27 May, 29 August–1 September
National Taiwan University, Taiwan, 30 September–28 November
Nion, U.S.A., 24 October

Scope of Research

Crystallographic and electronic structures of materials and their transformations are studied through direct imaging of atoms or molecules by high-resolution electron spectromicroscopy which realizes energy-filtered imaging and electron energy-loss spectroscopy as well as high resolution imaging. By combining this with scanning probe microscopy, the following subjects are urging: direct structure analysis, electron crystallographic analysis, epitaxial growth of molecules, structure formation in solutions, and fabrication of low-dimensional functional assemblies.

KEYWORDS

TEM EELS
STEM SPM
Cryo-TEM



Selected Publications

Kobayashi, T.; Ogawa, T.; Moriguchi, S.; Suga, T.; Yoshida, K.; Kurata, H.; Isoda, S., Inhomogeneous Substitution of Polyhalogenated Copper-phthalocyanine Studied by High-resolution Imaging and Electron Crystallography, *J. Electron Microsc.*, **52**, 85-90 (2003).
Minari, T.; Nemoto, T.; Isoda, S., Temperature and Electric-field Dependence of the Mobility of a Single-grain Pentacene Field-effect Transistor, *J. Appl. Phys.*, **99**, 034506 (2006).
Kiyomura, T.; Nemoto, T.; Ogawa, T.; Minari, T.; Yoshida, K.; Kurata, H.; Isoda, S., Thin-Film Phase of Pentacene Film Formed on KCl by Vacuum Deposition, *Jpn. J. Appl. Phys.*, **45**, 401-404 (2006).
Haruta, M.; Yoshida, K.; Kurata, H.; Isoda, S., Atomic Resolution ADF-STEM Imaging of Organic Molecular Crystal of Halogenated-Cu-phthalocyanine, *Ultramicroscopy*, **108**, 545-551 (2008).
Haruta, M.; Kurata, H.; Komatsu, H.; Shimakawa, Y.; Isoda, S., Site-resolved Oxygen K-edge ELNES of Layered Double Perovskite $\text{La}_2\text{CuSnO}_6$, *Physical Review B*, **80**, 165123 (2009).

Local Electronic Structure Analysis for Brownmillerite $\text{Ca}(\text{Sr})\text{FeO}_{2.5}$ Using Site-resolved Energy-loss Near-edge Structures

Oxygen K-edge and Fe $L_{2,3}$ -edge electron energy-loss near-edge structures (ELNES) were measured for FeO_6 octahedra and FeO_4 tetrahedra in the brownmillerite $\text{Ca}(\text{Sr})\text{FeO}_{2.5}$ by focusing an electron probe at individual Fe sites using scanning transmission electron microscopy (STEM) combined with electron energy-loss spectroscopy (EELS). The observed site-resolved oxygen K-ELNES showed different features reflecting the local chemical bonding around the FeO_6 octahedra and FeO_4 tetrahedra. A pre-peak in the O K-edge spectra, which is attributed to a transition to an unoccupied O 2p band hybridized with the Fe 3d band, shows splitting in the spectrum of the FeO_6 octahedral site. Additionally, for the oxygen linking the octahedral and tetrahedral Fe sites in $\text{CaFeO}_{2.5}$, charge transfer was found to preferentially occur toward the tetrahedral Fe ions. In the case of $\text{SrFeO}_{2.5}$, charge transfer from the oxygen located in the *ac* plane was biased toward the tetrahedral Fe atoms. Based upon an analysis of the pre-peak intensity of the O K-ELNES, it was concluded that bonding between the oxygen and iron atoms at the tetrahedral site was more covalent in character than at the octahedral site. The strong covalent character of the tetrahedral sites would be one of the reasons for distortion in the FeO_6 octahedra in $\text{Ca}(\text{Sr})\text{FeO}_{2.5}$, as exhibited by an extension along the *b*-axis.

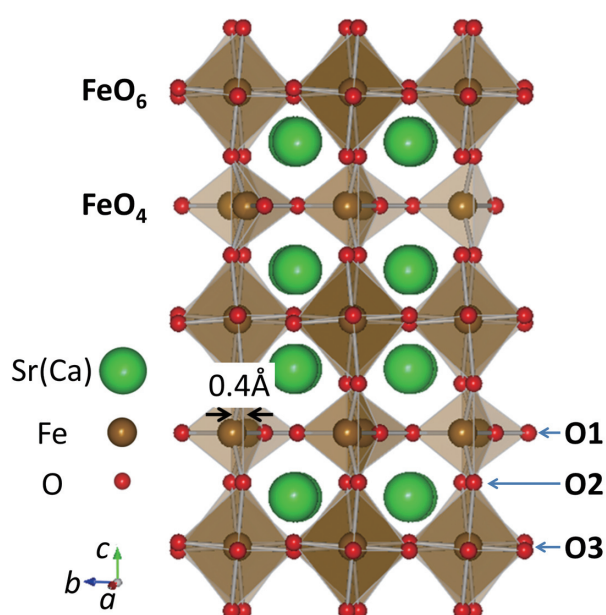


Figure 1. Structure model of brownmillerite $\text{Ca}(\text{Sr})\text{FeO}_{2.5}$. There are three nonequivalent oxygen atoms (O1, O2, and O3) in the unit cell.

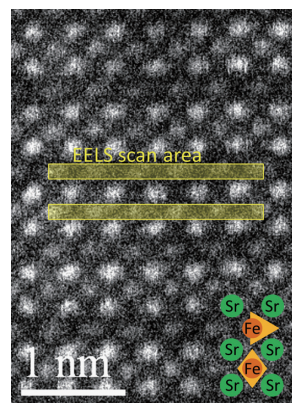
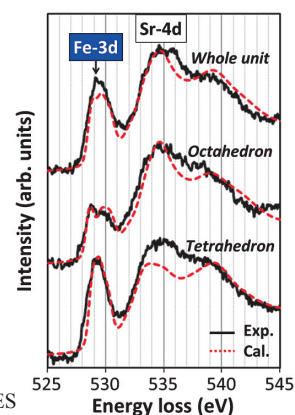


Figure 3. Site resolved O K-ELNES of $\text{SrFeO}_{2.5}$.

Figure 2. HAADF image of $\text{SrFeO}_{2.5}$.



Interface Structure of Gold Particles on TiO_2 Anatase

Gold particles supported on titanium dioxide (TiO_2) are known to activate many catalytic reactions. In this study, interface structure of gold on anatase was examined in the case on an anatase {101} surface, since the surface is the most important for several photocatalytic reactions. Anatase TiO_2 nanorods having clear washboard-like {101} outer surfaces were synthesized by using a double surfactants system. From high resolution electron microscopy observation for gold particle on the {101} surface, the (113) plane of gold was found to be parallel to the (101) surface of TiO_2 . Such an epitaxy is corresponding to be the axial and planar orientations of $[03\cdot1] (200)\text{Au} // [-31\cdot1] (113)\text{TiO}_2$, being originated from the smallest lattice mismatching, instead of the previous cases of $[01\cdot1] (111)\text{Au} // [02\cdot1] (112)\text{TiO}_2$ on the {110} and {112} surfaces of anatase TiO_2 .

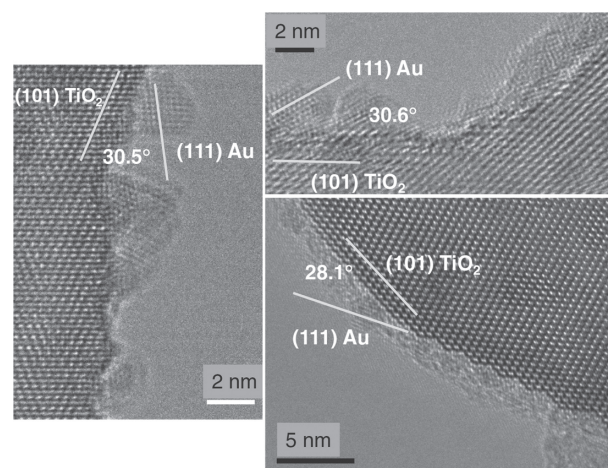


Figure 4. HR-TEM images of Au particles on {101} surfaces of anatase TiO_2 nanorods.